NJC

Accepted Manuscript

This is an *Accepted Manuscript*, which has been through the Royal Society of Chemistry peer review process and has been accepted for publication.

Accepted Manuscripts are published online shortly after acceptance, before technical editing, formatting and proof reading. Using this free service, authors can make their results available to the community, in citable form, before we publish the edited article. We will replace this *Accepted Manuscript* with the edited and formatted *Advance Article* as soon as it is available.

You can find more information about *Accepted Manuscripts* in the Information for Authors.

Please note that technical editing may introduce minor changes to the text and/or graphics, which may alter content. The journal's standard Terms & Conditions and the Ethical guidelines still apply. In no event shall the Royal Society of Chemistry be held responsible for any errors or omissions in this *Accepted Manuscript* or any consequences arising from the use of any information it contains.

ROYAL SOCIETY OF CHEMISTRY

www.rsc.org/njc

The modification of Ag_3VO_4 with graphene-like MoS_2 for the enhanced visible- light photocatalytic property and stability

Tingting Zhu[a], Liying Huang[a], Yanhua Song[b], Zhigang Chen[a], Haiyan Ji[a], Yeping Li[a], Yuanguo Xu[a], Qi Zhang[c], Hui Xu[a]*, Huaming Li[a]*

[a] Institute for Energy Research, School of Chemistry and Chemical Engineering, Jiangsu University, Zhenjiang 212013, P. R. China
[b] School of Environmental and Chemical, Engineering, Jiangsu University of Science and Technology, Zhenjiang 212003, P. R. China
[c] Hainan Provincial Key Lab of Fine Chemistry, Hainan University, Haikou, Hainan 570228, P.R. China
E-mail address: xh@ujs.edu.cn, lihm@ujs.edu.cn

A B S T R A C T

The graphene-like MoS_2 photocatalysts were synthesized by hydrothermal method. The obtained graphene-like MoS_2/Ag_3VO_4 composites were characterized by a series of means to demonstrate the structure and property. Owing to the elevated photogenerated electron separation and strong hole oxidizability as well as light harvesting, the obtained graphene-like MoS_2/Ag_3VO_4 composites displayed enhancing property for the degradation of methylene blue (MB) and rhodamine B (RhB) by comparing with the pure Ag_3VO_4 under visible light illumination. The degradation kinetics of graphene-like MoS_2/Ag_3VO_4 composites on MB and RhB were built to demonstrate the excellent photocatalytic activities. The measurement of electrochemical impedance spectroscopy (EIS) Nyquist plots was carried out to research the electron transfer and recombination processes of graphene-like MoS_2/Ag_3VO_4 composite. The possible photocatalytic mechanism of graphene-like MoS_2/Ag_3VO_4 composites was discussed by operating the active species trapping

experiments. The result showed the formative interface between graphene-like MoS_2 and Ag_3VO_4 accelerated the electron transfer performance.

Keywords: Graphene-like MoS_2, Ag_3VO_4, Photocatalytic, Composites

1. Introduction

Semiconductor photocatalysts have received extensive attention in consequence of their superior physical and chemical property as well as potential applications in dye degradation.[1-4] Among these semiconductor photocatalysts, TiO_2 has been regarded as the representative material due to its outstanding photocatalytic performance under UV-illumination, non-toxicity, and standing stability.[5-6] Nevertheless, the slight sunlight utilization limited its actual practice in environmental governance. In order to take adequate advantage of abundant spontaneous sunlight, a large number of green, sustainable and visible-light responsive photocatalysts were triumphantly researched. For instance: oxide-based,[7,8] Bi-based,[9,10] graphene-based,[11,12] and Ag-based[13,14] semiconductor photocatalysts.

Recently, keen interest has expressed in two-dimensional layered materials including graphene.[15] Despite it possesses unique properties, if anything, the zero band-gap energy of graphene makes it seem to be unfit for many optics and electronics applications.[16] Graphene-like molybdenum disulfide exhibits distinct difference from graphene. Graphene-like Molybdenum disulfide (MoS_2), with its inherent structure of S-Mo-S atom layers combined together through the van der Waals interaction, innate band gap, high carrier mobility as well, has shown broad prospects in these applications.[17,18] The distinct property of graphene-like MoS_2

makes it an advantageous candidate for the composite with other materials to enhance the photocatalytic activities. In recent years, the modification of semiconductor photocatalysts with graphene has exploited new prospect in scientific breakthrough and meaningfully extended the application of graphene.[19,20] After modifying successfully, the improved properties occurred resulting from the interface interaction. Immediately following the graphene, the method of modifying semiconductor photocatalysts with graphene-like MoS_2 to form composite to further enhance the photocatalytic properties of the photocatalysts has also been developed and has been demonstrated a promising strategy. For instance, in the MoS_2/Bi_2MoO_6,[21] MoS_2/CdS [22] and MoS_2/Ag_3PO_4[23] systems, the composites exhibited enhanced visible-light photocatalytic activities compared with the pure Bi_2MoO_6, CdS and Ag_3PO_4, respectively.

It was universally accepted that, Ag_3VO_4 indicated photocatalytic properties for pollutants decomposing and water splitting.[24-26] However, the practical application was limited due to its high recombination and low adsorption.[27] Based on the previous reports, modifying Ag_3VO_4 with other photocatalysts could restrain the recombination of pure Ag_3VO_4 and further enhance the photocatalytic activity.[28,29] Hence, in view of the advantage of graphene-like MoS_2, the graphene-like MoS_2/Ag_3VO_4 composite was designed in order to further improve the photocatalytic activity and stability of Ag_3VO_4 photocatalyst.

In this work, a simple and facile two-step method was reported for the synthesis of graphene-like MoS_2/Ag_3VO_4 composites at room temperature. The obtained

graphene-like MoS_2/Ag_3VO_4 composites were acted as photocatalysts for the visible-light degradation of methylene blue (MB) and rhodamine B (RhB). Besides, the effect of graphene-like MoS_2 content in the composites has been studied on photodegradation efficiency. Additionally, the possible mechanism for photocatalytic degradation of the dyes over graphene-like MoS_2/Ag_3VO_4 composites was discussed depending on the data available.

2. Experimental

2.1. Synthesis of the samples

All the materials used in the experiment were commercially purchased and without further purification.

Synthesis of graphene-like molybdenum disulfide (MoS_2): Molybdenum trioxide (MoO_3), potassium thiocyanate (KSCN) and deionized water were put into the polyethylene reactor.[30] The mixture was heated in the drying oven at 180℃ for 24 h after ultrasonic dispersion and magnetic stirring. The reactor was drawn out from the drying oven when the reaction accomplished and was naturally cooled to the room temperature. Afterwards, the mixture was centrifuged via high-speed centrifugal machine, baptized by deionized water and ethyl alcohol. After being dried at 60℃ for 6h, the obtained black powder was graphene-like MoS_2.

Synthesis of graphene-like MoS_2/Ag_3VO_4: A given quantity of graphene-like MoS_2 was put in aqueous solution by ultrasonic dispersion for 0.5 h. After that, under the condition of temperature controlling and magnetic stirring, $AgNO_3$ was added to the before-mentioned solution for 0.5 h. Then the prepared $Na_3VO_4 \cdot 12H_2O$

aqueous solution was dropwised into the aforementioned suspension by stirring for 4 h. Ultimately, the obtained graphene-like MoS_2/Ag_3VO_4 composites were gathered by the means of filtration, lavation and stoving. The individual Ag_3VO_4 was acquired in the absence of graphene-like MoS_2 through the same process.

2.2. Characterization

The X-ray diffraction (XRD) was recorded with a Bruker D8 diffractometer using Cu-Kα radiation (λ=1.5418 Å) in a scanning area of 2θ = 10-80° with the purpose of certifying the crystalline phase constituent and purity. The X-ray photoelectron spectra (XPS) were manipulated on a VG MultiLab 2000 system in order to testify the surface elements. The Fourier transform infrared spectroscopy (FT-IR) spectra were characterized by a Nicolet Model Nexus 470 FT-IR equipment. The transmission electron microscopy (TEM) image was performed on a JEOL-JEM-010 electron microscope. UV–vis diffuse reflectance spectra (DRS) were recorded on a UV–vis spectrophotometer (Shimadzu UV-2450, Japan) using $BaSO_4$ as the reflectance standard material. The energy-dispersive spectrometry (EDS) elemental mapping analysis was recorded on an energy-dispersive X-ray spectrometer fixed on to the FE-SEM apparatus, affirming the dimensional distribution of the elements for the graphene-like MoS_2/Ag_3VO_4 composites.

2.3. Photocatalytic tests

The photodegradation of MB (RhB) in an aqueous solution was operated under visible light irradiation at 30℃ employing a 300 W xenon lamp and 400 nm cutoff filter. In each test, 0.05 g of the sample was added to a Pyrex reactor with 100 mL of

MB (10 mg/ L) or RhB (10 mg/L) aqueous solution, which was cooled down by recycled water for the sake of impairing the impact of thermocatalytic. Before illumination, the suspensions were stirred for 1 h to achieve the sorption equilibrium. During the whole photoreactions, the MB (RhB)–photocatalyst solution was sustaining magnetically stirred, and 3 mL of the suspension was taken from the sample at 3 (5) min intervals. Then, the supernatant was extracted while the suspension was centrifuged by high-speed centrifugal machine for 3 min. After that, the supernatant was analyzed via measuring the absorbance at 664 nm for MB (553 nm for RhB) on a Shimadzu UV-2450 spectrophotometer. C/C_0 is the ratio of surplus dye concentration to the original concentration. The recycling experiment was conducted over the MB photodegradation under visible light irradiation to evaluate the stability of the graphene-like MoS_2/Ag_3VO_4 composites. After one reaction, the solution with photoc atalyst was centrifuged, washed, dried, and then sealed for the next run.

2.4 **Photoelectrochemical measurements**

The Electrochemical impedance characterization was measured by a CHI660B electrochemical analysis apparatus. The preparation process of the sample: Firstly, conductive glasses were put into a beaker with alcohol by ultrasonic treatment for 1 h. After air drying, they were intertwined by scotch tape at the leading end; secondly, the as-synthesized catalysts were put into the mixed solution of alcohol and ethanediol by ultrasonic treatment for 0.5 h. Then, the catalysts were dropwised to the conductive glasses using microsyringe; Additionally, the as-synthesized samples linked with conductive tapes were put into 5 mL $K_3Fe(CN)_6$ (3 mM) buffer solution, together with

platinum wire electrode and calomel electrode.

3. Results and discussion

Graphene-like MoS_2 modified Ag_3VO_4particles were synthesized by a simple and facile two-step method. The structure, elemental composition, morphology and optical absorption ability were characterized. Methylene blue (MB) and rhodamine B (RhB) dyes were used as model organic contaminants to evaluate the photoactivity of the graphene-like MoS_2/Ag_3VO_4 composites under visible light irradiation. The formative interface between graphene-like MoS_2 and Ag_3VO_4 accelerated the electron transfer performance and enhance the photoactivity of the composites..

3.1. Structure, elemental composition, morphology

The XRD patterns of the samples were characterized to verify the crystal phase structure and purity. Fig. 1 indicated the powder XRD patterns of the graphene-like MoS_2, Ag_3VO_4 and graphene-like MoS_2/Ag_3VO_4 composites. It was discovered that pure MoS_2 had two strong peaks at $2\theta = 32.8°$ and 58.0°corresponding to (100) and (110) diffraction planes of molybdenum disulfide (JCPDS 37-1492),[31] respectively. However, the peak at $2\theta = 14.5°$ (0 0 2) of the graphene-like MoS_2 could not be found, which manifested that the layers restacking did not occurre in syhthetic process and the poor crystallinity.[23] By comparison, the XRD patterns of graphene-like MoS_2/Ag_3VO_4 composites could be indexed to the structure of the individual Ag_3VO_4 (JCPDS No. 43-0542). Nevertheless, no representative diffraction peaks of graphene-like MoS_2 were observed in the graphene-like MoS_2/Ag_3VO_4 composites resulting from the low content of graphene-like MoS_2. The characterization of FT-IR,

XPS and TEM were carried out to further analyze the constituent of the graphene-like MoS_2/Ag_3VO_4 composites.

The chemical structure of the graphene-like MoS_2/Ag_3VO_4 catalysts was further demonstrated by FT-IR. Fig. 2 exhibited the FT-IR spectra of graphene-like MoS_2/Ag_3VO_4 composites with divergent content of graphene-like MoS_2. It could be apparently seen the main typical peaks of the pure graphene-like MoS_2 sample. The peaks positioned at 800-1700 cm^{-1} corresponding to the literature by Maugé et al.[32] For the pure Ag_3VO_4, the peaks at 501 cm^{-1} and 685 cm^{-1} were put down to the V-O-V stretching vibration,[33] the peaks located at 860 cm^{-1}, 895 cm^{-1}, 924 cm^{-1} and 966 cm^{-1} could be attributed to the silver vanadates,[34] the peaks at 924 cm^{-1} and 966 cm^{-1} were assigned to the VO_3 groups of the VO_4^{3-} tetrahedral.[35] The main diffraction peaks of the individual Ag_3VO_4 arose in the graphene-like MoS_2/Ag_3VO_4 composites after introducing the graphene-like MoS_2. Regarding to graphene-like MoS_2/Ag_3VO_4, the peak at 1630 cm^{-1} and 920 cm^{-1} occurred in the composite with the increasing content of the graphene-like MoS_2. Besides, the intensity of the peak at 1630 cm^{-1} for the 10 wt% graphene-like MoS_2/Ag_3VO_4 composite was clearly extruded and enhanced by making a comparison with other samples. It could be ascribed to the modification with graphene-like MoS_2 changing the chemical environment of Ag_3VO_4 or the overlay of the typical peaks for graphene-like MoS_2 and Ag_3VO_4. Depending on the investigation above, the conclusion that graphene-like MoS_2/Ag_3VO_4 composites included both graphene-like MoS_2 and Ag_3VO_4 could be drawn.

The XPS measurements were characterized to analyze the surface elements and the

atom bonding form of the graphene-like MoS_2/Ag_3VO_4 composites. Fig. 3a indicated the survey spectrum of the graphene-like MoS_2/Ag_3VO_4, which showed the coexistence of Mo, S, V, Ag and O elements without any impurities. The survey spectrum of the Ag_3VO_4 showed in Fig. S1a. Fig. 3b showed the high-resolution spectrum of Mo3d for the 7 wt% graphene-like MoS_2/Ag_3VO_4 composite. The peaks at about 232.6 eV and 235.7 eV for the 7 wt% graphene-like MoS_2/Ag_3VO_4 composite was homologous to Mo $3d_{3/2}$ and Mo $3d_{5/2}$ binding energies, respectively.[36,37] Fig. 3c showed the high-resolution spectrum of S2p for the 7 wt% graphene-like MoS_2/Ag_3VO_4 composite. The peaks at 161.7 eV and 162.6 eV were assigned to S $2p_{1/2}$ and S $2p_{3/2}$ binding energies, respectively.[38] Fig. 3b and 3c showed that existence of graphene-like MoS_2 in the graphene-like MoS_2/Ag_3VO_4 composite. In Fig. 3d, the peaks at 368.1 eV an 374.1 eV for the 7 wt% graphene-like MoS_2/Ag_3VO_4 composite respectively corresponded to Ag $3d_{5/2}$ and Ag $3d_{3/2}$ binding energies, which were higher than that of the pure Ag_3VO_4 (367.9 eV and 374.0 eV (Fig. S1b)). In Fig. 3e, the peaks at 524.1 eV and 516.6 eV for the 7 wt% graphene-like MoS_2/Ag_3VO_4 composite respectively corresponded to V $2p_{1/2}$ and V $2p_{3/2}$ binding energies, which were higher than that of the individual Ag_3VO_4 (516.6 eV and 524.1 eV (Fig. S1c)). The change could be assigned to the introduction of graphene-like MoS_2. In Fig. 3f, the peaks at 530.1 for 7 wt% graphene-like MoS_2/Ag_3VO_4 composite was higher than that of the Ag_3VO_4 (530.0 eV (Fig. S1d)).

The morphology and microstructure of as-prepared samples surveyed by the scanning electron microscopy (SEM) and transmission electron microscopy (TEM)

were displayed in Fig. 4, respectively. Fig. 4a revealed that plenty of irregularly shaped particles either distributed on the relatively smooth surface of the graphene-like MoS_2 sheets or scattered outside. The SEM images of the pure graphene-like MoS_2 and Ag_3VO_4 were indicated in Fig. S2. Fig. 3b showed that graphene-like MoS_2 had flower shapes with slice, indicating that graphene-like MoS_2 was suitable for surface modification. Fig. 3c showed that Ag_3VO_4 sample had an irregular particle with agglomerates. As observed in Fig. 3d, Ag_3VO_4 nano-particles dispersed on the surface of graphene-like MoS_2 or scattered outside. Fig. 3e showed that 7 wt% graphene-like MoS_2/Ag_3VO_4 composite contained the elements of Mo, S, V, O and Ag.

3.2. Optical absorption ability

Optical performance is of significant importance in the visible-light degradation of organic contaminant. Optical absorption of the individual graphene-like MoS_2, Ag_3VO_4 and graphene-like MoS_2/Ag_3VO_4 composites were investigated via UV-vis diffuse reflectance spectroscopy (UV-vis DRS). As observed in Fig. 5, graphene-like MoS_2 showed high absorption in visible region. The individual Ag_3VO_4 showed the photo-absorption property was the entire waveband, which suggested that an effective utilization of the solar source over Ag_3VO_4 could be acquired. Apparently, the absorption range of the graphene-like MoS_2/Ag_3VO_4 composites was impaired while compared with the individual Ag_3VO_4. Furthermore, with the increasing content of graphene-like MoS_2, blue shift took place in the composites. It should be attributed to the formation of heterostructure with the intervention of graphene-like MoS_2,

contributing to the improved photocatalytic properties and application in comprehensive environmental governance.

3.3. Photocatalytic performance

The photocatalytic activity of the as-obtained samples was evaluated via the removal of organic dyes. In this work, MB and RhB dyes were worked as the simulative contaminant. Fig. 6a exhibited the photocatalytic properties of the samples on MB degradation. It could be observed that, the photocatalytic performance of graphene-like MoS_2/Ag_3VO_4 composites was superior to that of the individual graphene-like MoS_2 and Ag_3VO_4 after 18 min of visible-light irradiation. Additionally, the photocatalytic activities of the graphene-like MoS_2/Ag_3VO_4 composites indicated apparent promotion in the wake of the graphene-like MoS_2 amount in the composites increasing from 0 to 1 wt%, 4 wt%, 7 wt% and 10 wt%. 7 wt% graphene-like MoS_2/Ag_3VO_4 reflected the optimal activity: almost 91% MB was decomposed within 18 min under visible light illumination. Yet, the removal of MB for graphene-like MoS_2, Ag_3VO_4, 1 wt%, 4 wt% and 10 wt% graphene-like MoS_2/Ag_3VO_4 composites was 32%, 23%, 52%, 75% and 85%, respectively. In consequence, the appropriate modified amount of graphene-like MoS_2 could enhance the photocatalytic activity in the maximum limit. On the basis of Fig. 6b, the degradation efficiency of RhB gradually heightened with the extension of visible light exposure time. Comparing to the individual graphene-like MoS_2 and Ag_3VO_4, graphene-like MoS_2/Ag_3VO_4 composites had enhanced photocatalytic activities under the visible light irradiation within 30 min: the photocatalytic degradation of RhB for graphene-like MoS_2,

Ag_3VO_4, 1 wt%, 4 wt%, 7 wt% and 10 wt% graphene-like MoS_2/Ag_3VO_4 was about 1%, 17%, 72% and 81wt%, respectively. Similarly, the results showed that 7 wt% graphene-like MoS_2/Ag_3VO_4 composite was the optimal proportion, indicating that the content of graphene-like MoS_2 affected photocatalytic activity of the composite. Nevertheless, when graphene-like MoS_2 content increased above 7 wt%, the photocatalytic efficiency decreased, although it remained higher than that of pure Ag_3VO_4. When the content of graphene-like MoS_2 exceeded 7 wt%, the excessive deposition of graphene-like MoS_2 clusters blocked the light photons and covered the active sites on the of Ag_3VO_4. More graphene-like MoS_2 might reduce the electron transfer efficiency of the photoinduced electrons from Ag_3VO_4 nanoparticles to graphene-like MoS_2, so the activity decreased under visible light irradiation. [39,40] Therefore, the proper content of graphene-like MoS_2 played a vital role in the enhancement of the photocatalytic activity.

The absorption spectral patterns of the samples were measured to further demonstrate the photocatalytic activity of 7 wt% graphene-like MoS_2/Ag_3VO_4 composite. In comparison with the pure Ag_3VO_4 (Fig. 7a), the absorption for MB of 7 wt% graphene-like MoS_2/Ag_3VO_4 composite (Fig. 7b) had substantially declined as the prolonging of the irradiation time. Similar results for the absorption of RhB. The maximum absorption wavelength of MB and RhB appeared a blue shift, which ascribed to the decomposition of chromophoric group in the aromatic structures.[41]

The degradation kinetics of graphene-like MoS_2/Ag_3VO_4 composites on MB and RhB were built to further demonstrate the enhanced photocatalytic activities. The

installed experimental data were required to comply to the first order model using a reduced Langmuir-Hinshelwood model. The equation $-Ln(C_t/C_0)=kt$ could be gained through integrating the formula $-dc/dt=kc$. Among which, C_0 represents the adsorption equilibrium concentration for MB (RhB), C_t reflects concentration for MB (RhB) at the homologous reaction time t, as well as k expresses the reaction rate constant. Evidently, the photocatalytic degradation rate of every composite was superior to that of the pure Ag_3VO_4 under visible light illumination, especially for 7 wt% graphene-like MoS_2/Ag_3VO_4 composite (Fig. 8). As observed in Table1 and Table 2, the k value of 7 wt% graphene-like MoS_2/Ag_3VO_4 for MB and RhB photodegradation were 10.31 times and 9.00 times of that of the individual Ag_3VO_4, respectively. The result indicated that the modification of Ag_3VO_4 with graphene-like MoS_2 could improve the photocatalytic activity.

3.4. Possible photocatalytic mechanisms

As is well-known, the photocatalytic activity of the catalyst was influenced by the transfer process of the photo-generated electron. The Electrochemical impedance spectroscopy (EIS) Nyquist plots of as-obtained samples were characterized to investigate the electron transport and recombination processes. Fig. 9 showed the electrochemical impedance spectroscopy (EIS) Nyquist plot of the pure Ag_3VO_4, graphene-like MoS_2 and 7 wt% graphene-like MoS_2/Ag_3VO_4 composite. Given the preparation of electrolyte and electrodes, the semicircle with high frequency was homologizing to the resistance of the electrodes.[42] Obviously, 7 wt% graphene-like MoS_2/Ag_3VO_4 composite presented a comparatively smaller arc radius under visible

light illumination, whereas the pure Ag_3VO_4 and graphene-like MoS_2 presented a larger arc radius. Consequently, the restrained recombination of electron had taken place in 7 wt% graphene-like MoS_2/Ag_3VO_4 composite. Namely, effective segregation of photoproduced electron-hole pairs and enhanced photocatalytic activity was showed as the intervention of graphene-like MoS_2 into Ag_3VO_4.

Based on the analyses above, the outstanding photocatalytic activity of graphene-like MoS_2/Ag_3VO_4 composites could be attributed to the interface interaction and charge transport between graphene-like MoS_2 and Ag_3VO_4. The efficiency for separating the photogenerated electron-holes, oxidation capability of the holes and band gap might account for the photocatalytic activity.[43,44]

Two scavengers were taken to probe the reactive species on the purpose of further understanding the reaction mechanisms. In this research, t-BuOH played the part of hydroxyl radical scavenger,[45] and EDTA-2Na played the part of holes scavenger.[46,47] The transfusion of hydroxyl radical scavenger mildly retarded the degradation efficiency of MB for the 7 wt% graphene-like MoS_2/Ag_3VO_4 composite (Fig. 10). Nevertheless, the immission of EDTA-2Na absolutely hindered the photocatalytic property of the 7 wt% graphene-like MoS_2/Ag_3VO_4 composite with the radical holes were acquired. Similarly, the holes oxidation occupied the leading position in the photodegradation of RhB (Fig. S3). Consequently, it was rational to conclude that the hole oxidation was of vital importance in the photocatalytic degradation of MB and RhB dyes.

The cycling experiments were operated to investigate the stability and reusability of

the 7 wt% graphene-like MoS_2/Ag_3VO_4 composite over MB degradation under the visible light irradiation. The photocatalytic activity of 7 wt% graphene-like MoS_2/Ag_3VO_4 for the degradation of MB did not reduce observably after four cycling experiments (Fig. 11). Similarly, the cycling experiments of the 7 wt% graphene-like MoS_2/Ag_3VO_4 composite on RhB degradation showed that the photocatalytic activity did not alter apparently (Fig. S4). According to Fig. 12, it was obvious that the main typical peaks of the recycled 7 wt% graphene-like MoS_2/Ag_3VO_4 photocatalyst did not alter not only for FT-IR spectra but also for XRD patterns. Additionally, the structure of the 7 wt% graphene-like MoS_2/Ag_3VO_4 composite did not damage after the recycling degradation. Therefore, the as-synthesized 7 wt% graphene-like MoS_2/Ag_3VO_4 composite was reusable and stable.

According to numerous literatures, the enhancement of the photocatalytic activity could be due to the valid charge transfer on the surface of the two semiconductors (graphene-like MoS_2 and Ag_3VO_4).[48-50] Photocatalysts in view of semiconductor materials could genarate photoproduction electrons which have doughty reducibility and holes with doughty oxidizability under the illumination of visible light, resulting in the transformation of organic and inorganic contaminants into innocuous substance. Fig. 13 showed the photocatalytic mechanism chart of the graphene-like MoS_2/Ag_3VO_4 samples. The segregation of photogenerated electron-holes pairs occurred in the graphene-like MoS_2 semiconductor photocatalyst under visible light irradiation, concurrently, the photogenerated electrons diverted from VB (valence band) to the CB (valence band), contributing to the production of holes in the VB of

graphene-like MoS_2. E_{CB} coulde be calculated via Mulliken electrone gativity theory: $E_{CB}= \chi- Ec- 1/2$ Eg. Among which, E_{CB} is the conduction band edge energy, Ec is the energy of free electrons, χ is the absolute electro negativity, Eg is the band gap energy. The narrow band gap (Eg) for graphene-like MoS_2 is 1.8 eV. The X values for graphene-like MoS_2 is calculated to be 5.33 eV. The Ec for graphene-like MoS_2 is about 4.5 eV [51]. Therefore, the value of VB for graphene-like MoS_2 was predicted to be 1.78 eV. According to the $E_{VB} = E_{CB}+$ Eg, the value of CB of graphene-like MoS_2 was predicted to be -0.12 eV. The value of VB and CB for Ag_3VO_4 were calculated to be 2.24 eV and 0.04 eV, respectively [41,52]. Therefore, the electrons in the CB of graphene-like MoS_2 quickly transferred to the Ag_3VO_4 by means of the interface interaction because of the CB edge potential of graphene-like MoS_2 was negative than that of Ag_3VO_4, and afterwards diverted to the graphene-like MoS_2 photocatalyst again. The holes staying on the graphene-like MoS_2 effectively facilitated the supernal photo-oxidation efficiency. Towards photodegradation, the assimilation for the dye molecules over the catalyst played a significant role in improving the photodegradation efficiency. These chromophoric groups for the dye molecules were decomposed by the graphene-like MoS_2/Ag_3VO_4 photocatalysts under visible light irradiation when the organic dyes (MB and RhB) infiltrated onto the samples. Judging from the discussion above, the modification of Ag_3VO_4 with graphene-like MoS_2 could effectively promote the separated efficiency of electron-hole pairs, further boost the degradation efficiency of the dyes (MB and RhB) and photocatalytic activity under the visible light.

4. Conclusion

In summary, the graphene-like MoS_2/Ag_3VO_4 composites were synthesized in a simple and facile two-step method. The composites indicated remarkable promoted photocatalytic activities in methylene blue and rhodamine B degradation by making a comparison with the pure Ag_3VO_4 under visible light irradiation. Among all graphene-like MoS_2/Ag_3VO_4 composites, the 7 wt% graphene-like MoS_2/Ag_3VO_4 sample reflected the most outstanding photocatalytic activity and was regarded as the optimal proportion. The synergistic effects and electron divert between graphene-like MoS_2 and Ag_3VO_4 accounted for the outstanding photocatalytic activities. The cycling experiments surveyed the stability and reusability of graphene-like MoS_2/Ag_3VO_4 sample. The composite photocatalysts might have potential applications in sewage treatment.

Acknowledgements

The authors genuinely appreciate the financial support of this study from the National Nature Science Foundation of China (Nos. 21476097, 21476098, 21406094), Natural Science Foundation of Jiangsu Province (BK20130513, BK20140533), Postdoctoral Foundation of China (2014M551520) and A Project Funded by the Priority Academic Program Development of Jiangsu Higher Education Institutions.

References

1 S. Yang, L. Li, W. H. Yuan and Z. L. Xia, *Dalton Trans*., 2015, **44**, 6374-6383.

2 E. Kowalska, Z. Wei, B. Karabiyik, A. Herissan, M. Janczarek, M. Endo, A. Markowska-Szczupak, H. Remita and B. Ohtani, *Catal. Today*., 2015, **252**, 136-142.

3 Y. H. Ao, L. Y. Xu, P. F. Wang, C. Wang, J. Hou and J. Qian, *Dalton Trans*., 2015, **44**, 11321-11330.

4 L. Wei, Z. Y. Ma, G. Q. Bai, J. M. Hu, X. H. Guo, B. Dai and X. Jia, *Appl. Catal. B: Environ*., 2015, **174-175**, 43-48.

5 E. López Cuellar, A. Martínez-de la Cruz, N. Chávez Torres and J. Olivares Cortez, *Catal. Today*., 2015 , **252**, 2-6.

6 L. Y. Huang, H. Xu, Y. P. Li, H. M. Li, X. N. Cheng, J. X. Xia, Y. G. Xu and G. B. Cai, *Dalton Trans*., 2013, **42**, 8606-8617.

7 Y. -J. Yuan, F. Wang, B. Hu, H. -W. Lu, Z. -T. Yu and Z. -G. Zou, Dalton Trans., 2015, 44, 10997-11003.

8 S. C. Han, L. F. Hu, Z. Q. Liang, S. Wageh, A. A. Al-Ghamdi, Y. S. Chen and X. S. Fang, *Adv. Funct. Mater*., 2014, **24**, 5719-5727.

9 T. Yan, M. Sun, H. Y. Liu, T. T. Wu, X. J. Liu, Q. Yan, W. G. Xu and B. Du, *J. Alloys Compd*., 2015, 634, 223-231.

10 C. S. Chen, S. Y. Cao, W. W. Yu, X. D. Xie, Q. C. Liu, Y. H. Tsang and Y. Xiao, *J. Vac. Sci. Technol*. B 2015, **116**, 48-53.

11 L. M. Hu, S. Y. Dong, Q. L. Li, J. L. Feng, Y. Q. Pi, M. L. Liu, J. Y Sun and J. H. Sun, *J. Alloys Compd*., 2015, **633**, 256-264

12 J. Hu, H. S. Li, Q. Wu, Y. Zhao and Q. Z. Jiao, *Chem. Eng. J*., 2015, **263**, 144-150.

13 X. Lin, X. Y. Guo, W. L. Shi, F. Guo, H. J. Zhai, Y. S. Yan and Q. W. Wang, *Catal.Commun*., 2015, **66**, 67-72.

14 J. X. Wang, H. Ruan, W. J. Li, D. Z. Li, Y. Hu, J. Chen, Y. Shao and Y. Zheng, *J. Phys. Chem. C*, 2012, **116 (26)**, 13935-13943.

15 M. Chhowalla, H. S. Shin, G. Eda, L. -J. Li, K. P. Loh and H. Zhang, *Nat. Commun*. 2013, **5**, 263-275.

16 M. A. Ibrahem, T. -W. Lan, J. K. Huang, Y. -Y. Chen, K. -H. Wei, L. -J. Li, C. W. Chu, RSC Adv. 2013, **3**, 13193-13202.

17 D. Gopalakrishnan, D. Damien and M. M. Shaijumon, *ACS Nono*., 2014, **8**, 5297-5303.

18 L. J. Shen, M. B. Luo, Y. H. Liu, R. W. Liang, F. F. Jing and L. Wu, *Appl. Catal. B: Environ*., 2015, **166-167**, 445-453.

19 B. Pant, P. Pokharel, A. P. Tiwari, P. S. Saud, M. Park, Z. K. Ghouri, S. Choi, S. -J. Park and H. -Y. Kim, *Ceram. Int*., 2015, **141**, 5656-5662.

20 R. G. He, S. W. Cao, D. P. Guo, B. Cheng, S. Wageh, A. A. Al-Ghamdi and J. G. Yu, *Ceram. Int*., 2015, **41**, 3511-3517.

21 Y. J. Chen, G. H. Tian and Y. H. Shi, *Appl. Catal. B: Environ*., 2015, **164**, 40-47.

22 C. X. Wang, H. H. Lin and Z. Z. Xu, *RSC Adv*., 2015, **5**, 15621-15626.

23 P. F. Wang, P. H. Shi and Y. H. Hong, *Mater. Res. Bull*., 2015, **62**, 24-29.

24 X. Hu and C. Hu, *J. Solid State Chem*., 2007, **180**, 725-732.

25 R. Konta, H. Kato, H. Kobayashi and A. Kudo, *Phys. Chem. Chem. Phys*., 2003, **5**, 3061-3065.

26 L. Zhang, Y. M. He, P. Ye, Y. Wu and T. H. Wu, *J. Alloys Compd*., 2013, 549, 105-113.

27 D. P. Das, A. Samal, J. Das, A. Dash and H. Gupta, *Photochem. Photobiol*., 2013, **90**, 57-65.

28 K. Wangkawong, S. Phanichphant, D. Tantraviwat and B. Inceesungvorn, *J. Colloid Interface Sci*., 2015, **454**, 210-215.

29 L. Zhang, Y. M. He, P. Ye, Y. Wu and T. H. Wu, *J. Alloys Compd*., 2013, **549**, 105-113.

30 H. S. S. Ramakrishna Matte, A. Gomathi, A. K. Manna, D. J. Late, R. Datta, S. K. Pati and C. N. R. Rao, *Angew. Chem. Int. Ed*., 2010, **49**, 4059-4062.

31 K. Chang and W. X. Chen, *J. Mater. Chem*., 2011, **21**, 17175-17184.

32 F. Mauge, J. Lamotte and N. S. Nesterenko, *Catal. Today*., 2001, **70**, 271-284.

33 C. M. Huang, G. T. Pan, Y. C. M. Li, T. C. –K. Yang, *Appl. Cata. A: General*, 2009, **358**, 164-172.

34 M. Xue, J. Ge, H. Zhang, J. Shen, *Appl. Cata. A* 2007, **330**, 117-126.

35 S. Murugesan, A. Wijayasinghe, B. Bergman, *Solid State Ionics*, 2007, **178**, 779-783.

36 S. M. Cui , Z. H. Wen , X. K. Huang , J. B. Chang and J. H. Chen, *small*, 2015, **19**, 2305-2313.

37 J. Kibsgaard, Z. B. Chen, B. N. Reinecke and T. F. Jaramillo, *Nat. Mater*., 2012, **11**, 963.

38 Y. Huang, Y. Chen, C. Hu, B. Zhang, T. Shen, X. Chen and M. Q. Zhang, *J. Mater. Chem*., 2012, **22**, 10999-11002.

39 J. Xu and X. J. Cao, *Chem. Eng. J*., 2015, **260**, 642-648.

40 S. Kumar, T. Surenda and B. Kumar, *J. Mater. Chem A*., 2013, **1**, 5333-5340.

41 S. Wang, D. Li, C. Sun, S. Yang, Y. Guan and H. He, *Appl. Catal. B: Environ*., 2014, **144**, 885-892.

42 X. J. Bai, L. Wang, Y. J. Wang, W. Q. Yao and Y. F. Zhu, *Appl. Catal. B: Environ*., 2014,**152-153**, 2262-270.

43 M. Z. Zhong, Z. M. Wei, X. Q. Meng, F. M. Wu, J. B. Li, *Eur. J. Inorg. Chem*., 2014, 3245-3251.

44 X. Zhang, L. Zhang, J. -S. Hu, C. -L. Pan and C. -M. Hou, *Appl. Surf. Sci*., 2015, **346**, 33-40.

45 Q. Li, N. Zhang, Y. Yang, G. Z. Wang and D. H. L. Ng, *Langmuir*, 2014, **30**, 8965-8972.

46 Y. Zang, L. Li, X. Li, R. Lin and G. Li, *Chem. Eng. J*., 2014, **246**, 277-286.

47 S. Feng, H. Xu and L. Liu, *Colloids Surf. A*., 2012, **410**, 23-30.

48 C. J. Huang, J. L. Hu, S. Cong, Z. G. Zhao, X. Q. Qiu, *Appl. Catal. B: Environ*., 2015, **174-175**, 105-112.

49 Y. Hu, X. Song, S. M. Jiang and C. H. Wei, *Chem. Eng. J*., 2015, **274**, 102-112.

50 X. Li, X. Chen, H. Niu, X. Han, T. Zhang, J. Y. Liu, H. M. Lin and F. Y. Qu, *J. Colloid Interface Sci*., 2015, **452**, 89-97.

51 B. Weng, X. Zhang, N. Zhang, Z-R. Tang and Y-J. Xu, *Langmuir* 2015, **31**, 4314-4322.

52 J. Wang, P. Wang, Y. Cao, J. Chen, W. Li, Y. Shao, Y. Zheng and D. Li, *Appl. Cata.*

B., 2013, **136-137**, 94-102.

Table 1

Pseudo-first-order rate constant for MB photodegradation using different photocatalysts.

Photocatalysts	The first order kinetic equation	$k(min^{-1})$	R^2
1 wt% graphene-like MoS_2/Ag_3VO_4	$\ln(C/C_0)=-0.040t$	0.040	0.998
4 wt% graphene-like MoS_2/Ag_3VO_4	$\ln(C/C_0)=-0.076t$	0.076	0.996
7 wt% graphene-like MoS_2/Ag_3VO_4	$\ln(C/C_0)=-0.134t$	0.134	0.999
10 wt% graphene-like MoS_2/Ag_3VO_4	$\ln(C/C_0)=-0.108t$	0.108	0.999
Ag_3VO_4	$\ln(C/C_0)=-0.013t$	0.013	0.991

Table 2

Pseudo-first-order rate constant for RhB photodegradation using different photocatalysts.

Photocatalysts	The first order kinetic equation	$k(min^{-1})$	R^2
1 wt% graphene-like MoS_2/Ag_3VO_4	$\ln(C/C_0)=-0.016t$	0.016	0.992
4 wt% graphene-like MoS_2/Ag_3VO_4	$\ln(C/C_0)=-0.033t$	0.033	0.999
7 wt% graphene-like MoS_2/Ag_3VO_4	$\ln(C/C_0)=-0.054t$	0.054	0.999
10 wt% graphene-like MoS_2/Ag_3VO_4	$\ln(C/C_0)=-0.043t$	0.043	0.999
Ag_3VO_4	$\ln(C/C_0)=-0.006t$	0.006	0.995

Figure captions

Fig. 1. XRD patterns of samples: Ag_3VO_4 (a); 1 wt%, 4 wt%, 7 wt% and 10 wt% graphene-like MoS_2/Ag_3VO_4 composites (b, c, d, e); graphene-like MoS_2 (f).

Fig. 2. FT-IR spectra of the as-synthesis samples: Ag_3VO_4 (a); 1 wt%, 4 wt%, 7 wt% and 10 wt% graphene-like MoS_2/Ag_3VO_4 composites (b, c, d, e); graphene-like MoS_2 (f).

Fig. 3. XPS spectra of the samples: (a) the survey scan of the 7 wt% graphene-like MoS_2/Ag_3VO_4 composite; (b) Mo 3d, (c) S 2p, (d) Ag 3d (e) V 2p and (f) O 1s of the 7 wt% graphene-like MoS_2/Ag_3VO_4 composite.

Fig. 4. SEM images of 7 wt% graphene-like MoS_2/Ag_3VO_4 composites; TEM images of the samples: (a) pure MoS_2, (b) pure Ag_3VO_4, (c) 7 wt% graphene-like MoS_2/Ag_3VO_4 composites; (e) showed the energy-dispersive X-ray spectra (EDS) of the 7 wt% graphene-like MoS_{24}/Ag_3VO_4 composite.

Fig. 5. UV-vis diffuse reflectance spectra of the samples.

Fig. 6. Photocatalytic activities of as-synthesized samples for degradation of MB (a) and RhB (b) under visible-light irradiation.

Fig. 7. Absorption spectrum of MB with different irradiation times of Ag_3VO_4 (a) and 7wt% graphene-like MoS_2/Ag_3VO_4 (b) composite; absorption spectrum of RhB with different irradiation times of Ag_3VO_4 (c) and 7wt% graphene-like MoS_2/Ag_3VO_4 (d) composite

Fig. 8. The kinetics of photodegradation of MB (a) and RhB (b) for the samples

Fig. 9. Electrochemical impedance spectroscopy of the as-synthesized samples under visible light irradiation.

Fig. 10. Plots of photogenerated active species for the photodegradation of MB by 7wt% graphene-like MoS_2/Ag_3VO_4 composite under visible light illumination.

Fig. 11. Cycling runs of 7 wt% graphene-like MoS_2/Ag_3VO_4 composite for the degradation of MB under the visible light irradiation

Fig. 12. The XRD patterns (a) and FT-IR patterns (b) of used recycled 7 wt%

graphene-like MoS_2/Ag_3VO_4 sample

Fig. 13. Photocatalytic mechanism diagram of the graphene-like MoS_2/Ag_3VO_4 samples.

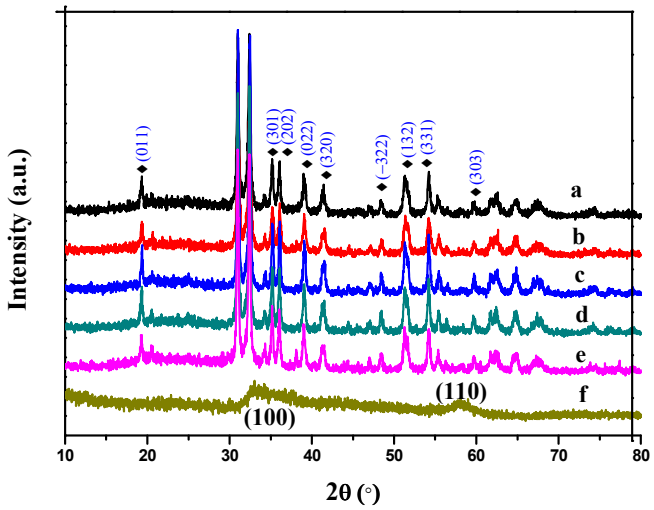

Fig. 1 XRD patterns of samples: Ag_3VO_4 (a); 1 wt%, 4 wt%, 7 wt% and 10 wt% graphene-like MoS_2/Ag_3VO_4 composites (b, c, d, e); graphene-like MoS_2 (f).

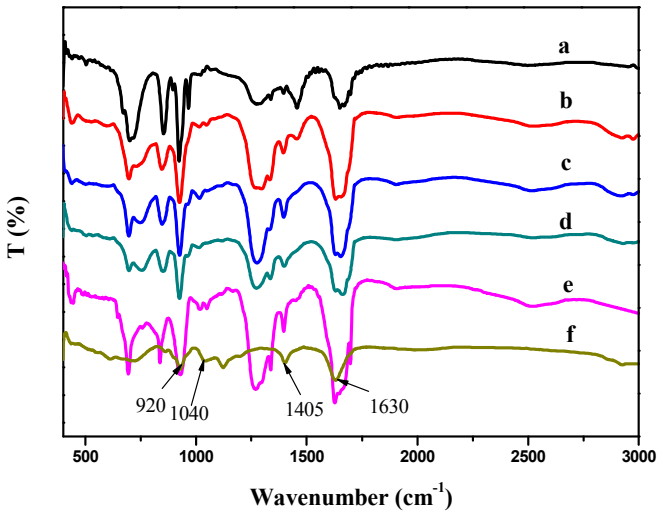

Fig. 2 FT-IR spectra of the as-synthesis samples: Ag_3VO_4 (a); 1 wt%, 4 wt%, 7 wt% and 10 wt% graphene-like MoS_2/Ag_3VO_4 composites (b, c, d, e); graphene-like MoS_2 (f).

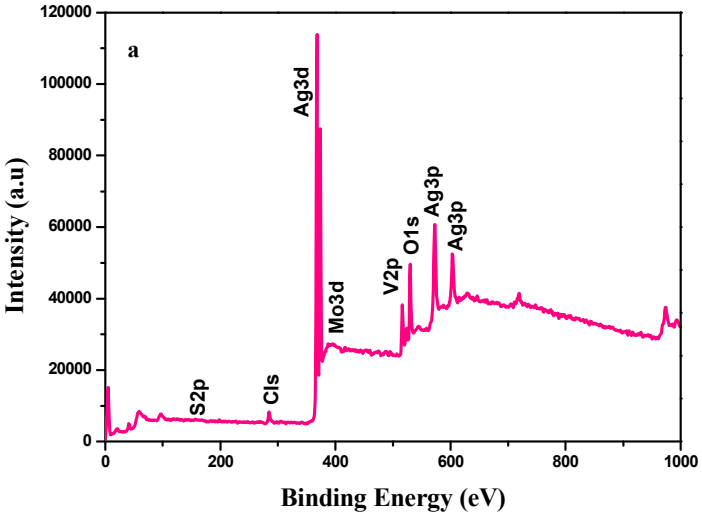

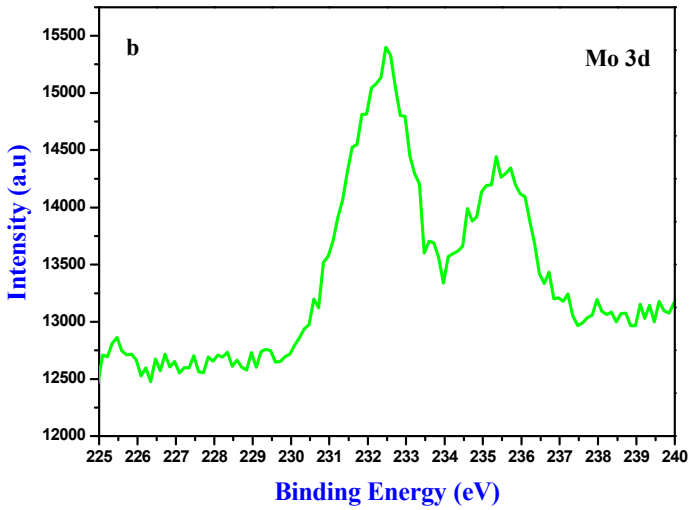

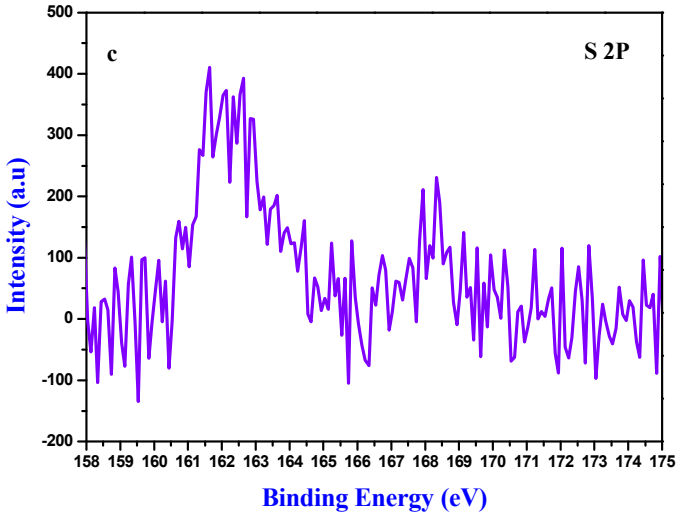

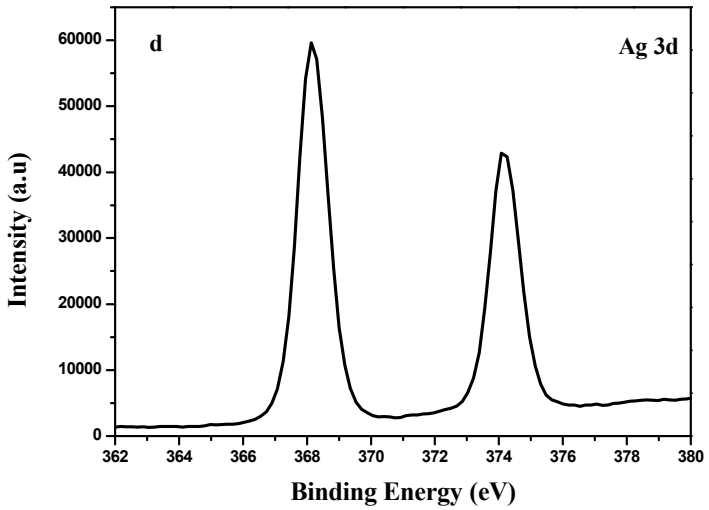

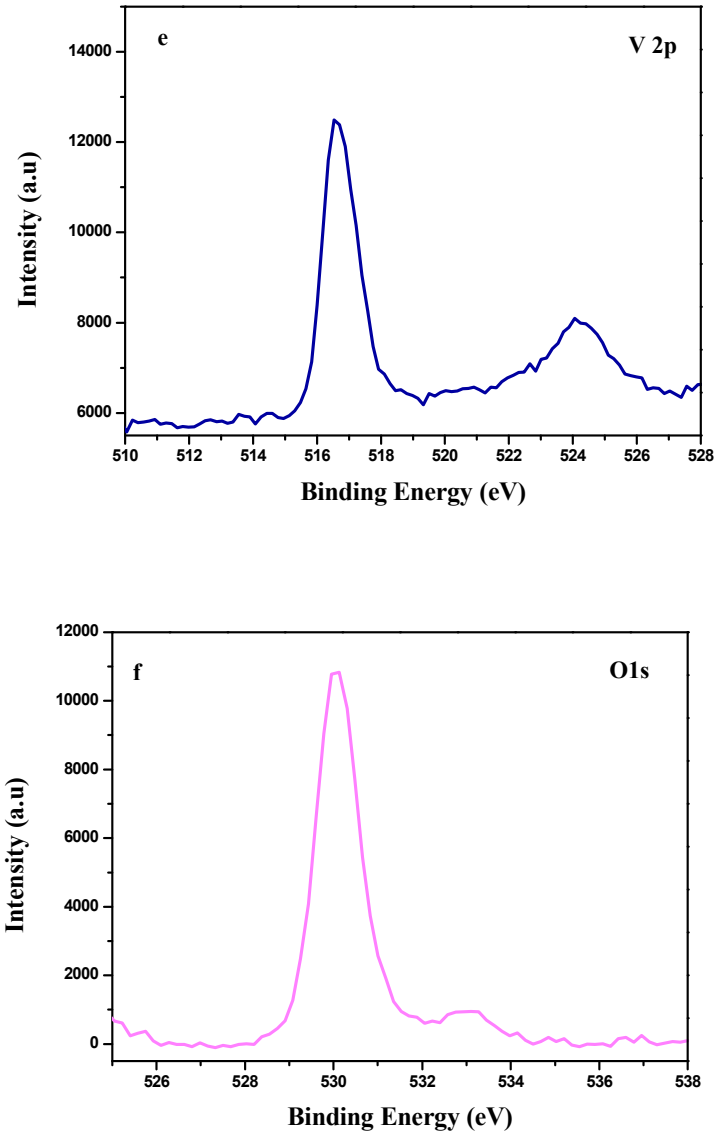

Fig. 3 XPS spectra of the samples: (a) the survey scan of the 7 wt% graphene-like MoS_2/Ag_3VO_4 composite; (b) Mo 3d, (c) S 2p, (d) Ag 3d (e) V 2p and (f) O 1s of the 7 wt% graphene-like MoS_2/Ag_3VO_4 composite.

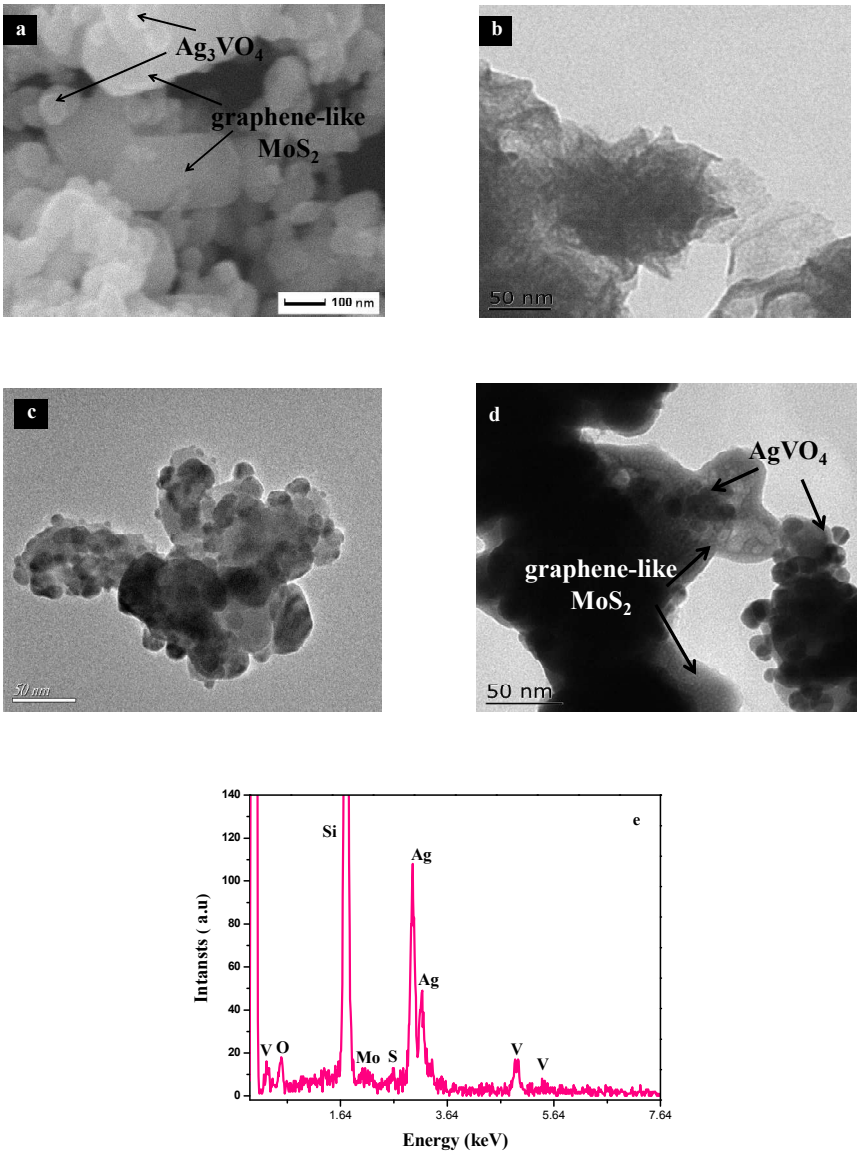

Fig. 4 SEM images of 7 wt% graphene-like MoS_2/Ag_3VO_4 composites; TEM images of the samples: (a) pure graphene-like MoS_2, (b) pure Ag_3VO_4, (c) 7 wt% graphene-like MoS_2/Ag_3VO_4 composite; (e) showed the energy-dispersive X-ray spectra (EDS) of the 7 wt% graphene-like MoS_{24}/Ag_3VO_4 composite.

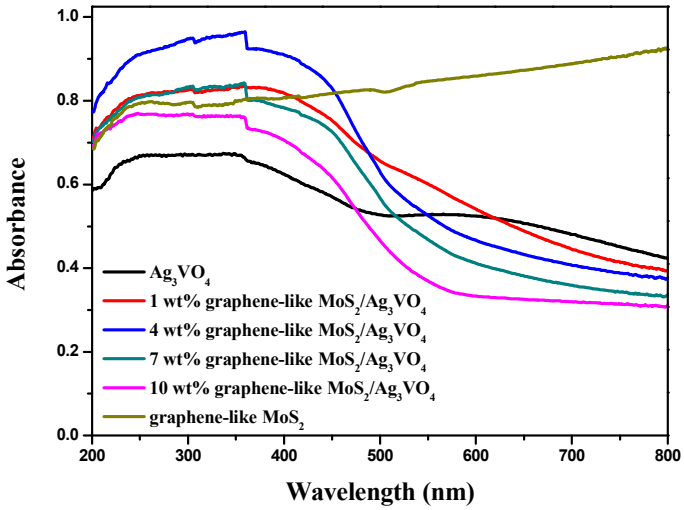

Fig. 5 UV-vis diffuse reflectance spectra of the samples.

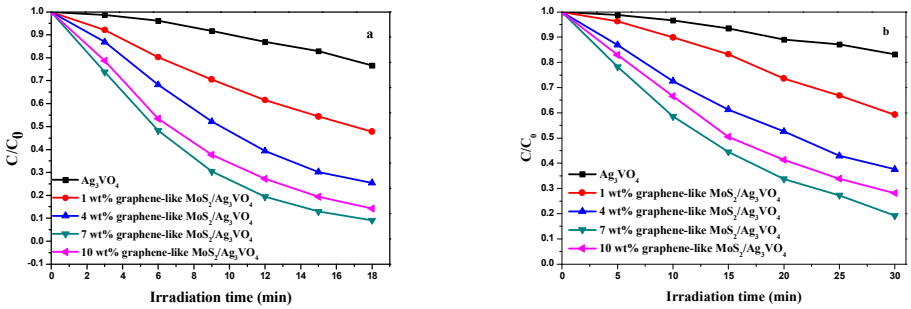

Fig. 6 Photocatalytic activities of as-synthesized samples for degradation of MB (a) and RhB (b) under visible-light irradiation.

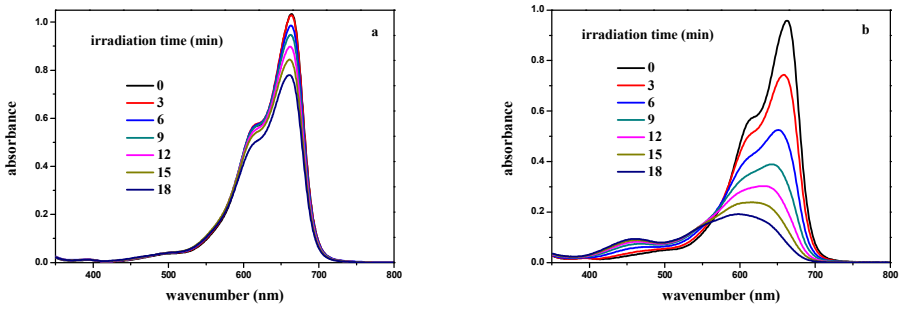

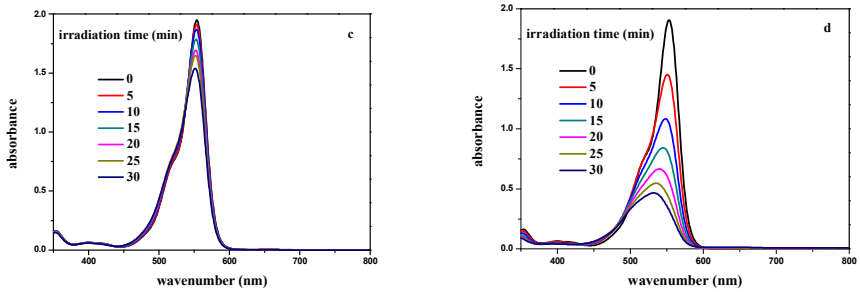

Fig. 7 Absorption spectrum of MB with different irradiation times of Ag_3VO_4 (a) and 7wt% graphene-like MoS_2/Ag_3VO_4 (b) composite; absorption spectrum of RhB with different irradiation times of Ag_3VO_4 (c) and 7wt% graphene-like MoS_2/Ag_3VO_4 (d) composite

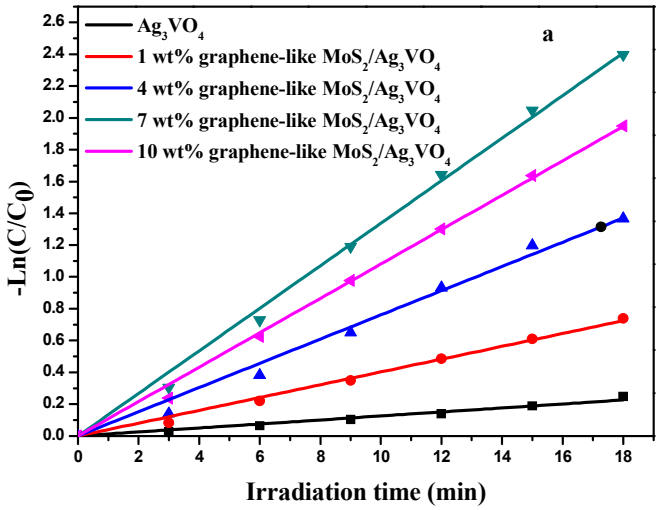

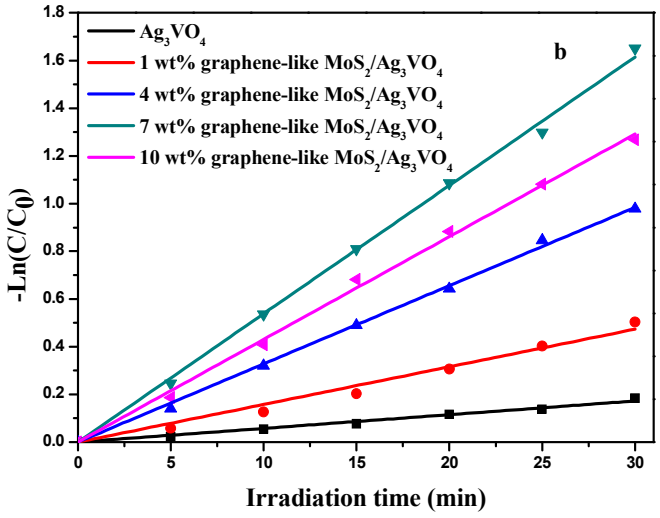

Fig. 8 The kinetics of photodegradation of MB (a) and RhB (b) for the samples

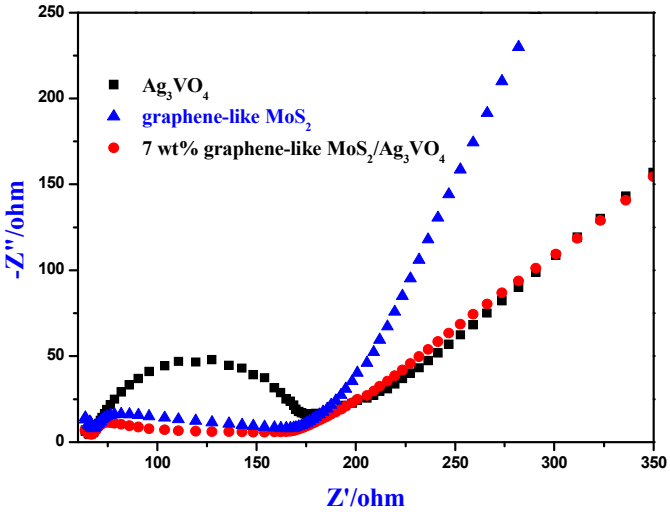

Fig. 9 Electrochemical impedance spectroscopy of the as-synthesized samples under visible light irradiation.

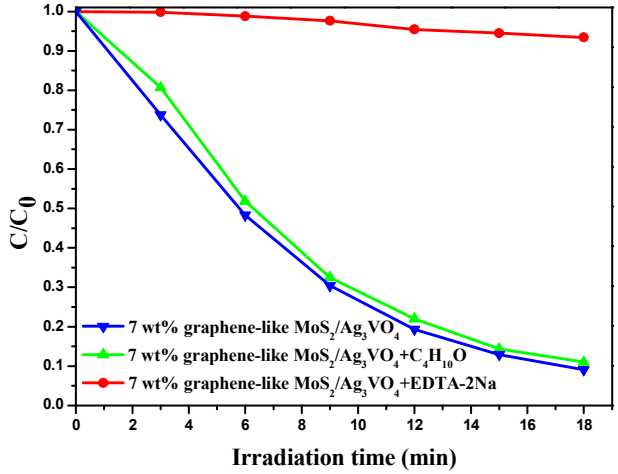

Fig. 10 Plots of photogenerated active species for the photodegradation of MB by 7wt% graphene-like MoS_2/Ag_3VO_4 composite under visible light illumination.

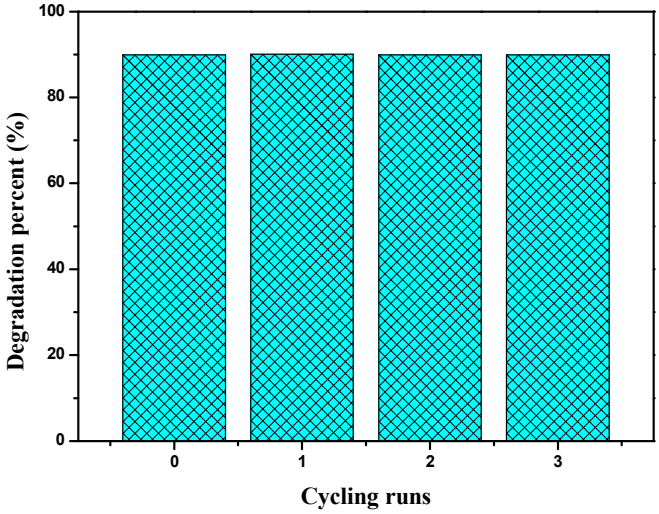

Fig. 11 Cycling runs of 7 wt% graphene-like MoS_2/Ag_3VO_4 composite for the degradation of MB under the visible light irradiation

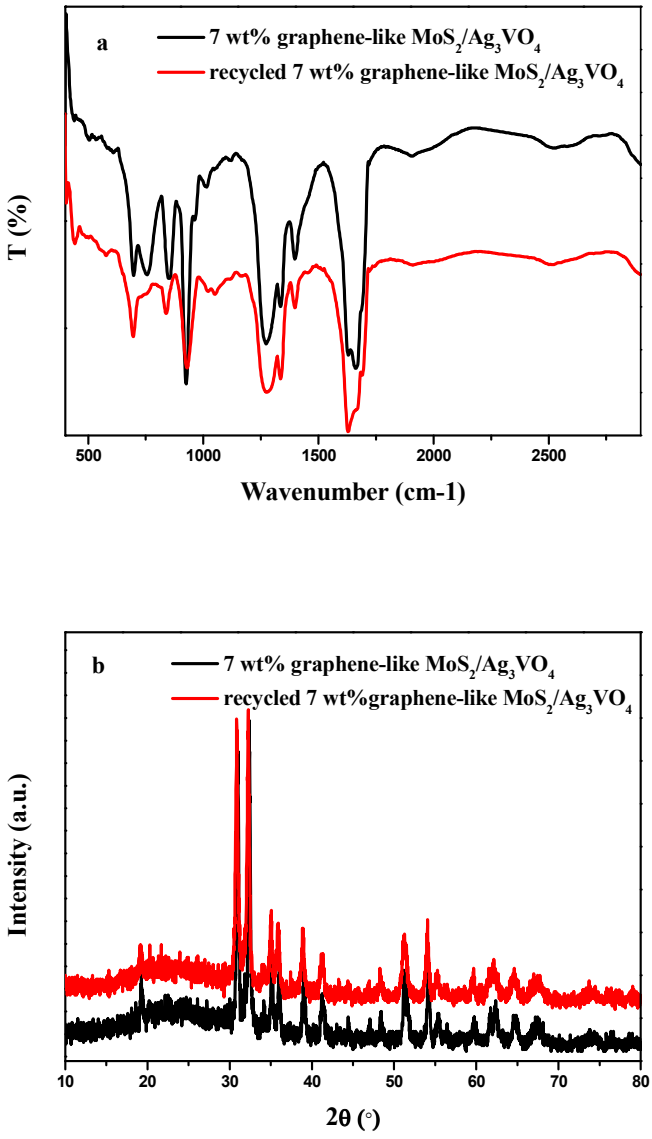

Fig. 12 The XRD patterns (a) and FT-IR patterns (b) of used recycled 7 wt% graphene-like MoS_2/Ag_3VO_4 sample

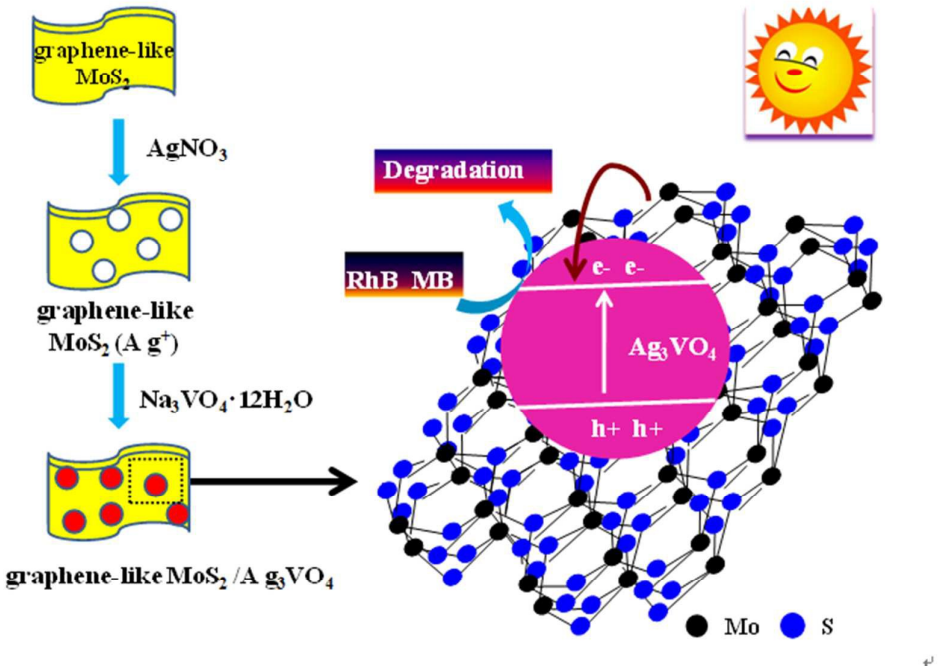

Fig. 13 Photocatalytic mechanism diagram of the graphene-like MoS_2/Ag_3VO_4 samples.

The modification of Ag_3VO_4 with graphene-like MoS_2 for the enhanced visible- light photocatalytic property and stability

Tingting Zhu[a], Liying Huang[a], Yanhua Song[b], Zhigang Chen[a], Haiyan Ji[a], Yeping Li[a], Yuanguo Xu[a], Qi Zhang[c], Hui Xu[a]*, Huaming Li[a]*

[a] School of Chemistry and Chemical Engineering, Institute for Energy Research, Jiangsu University, Zhenjiang 212013, P. R. China

[b] School of Environmental and Chemical, Engineering, Jiangsu University of Science and Technology, Zhenjiang 212003, P. R. China

[c] Hainan Provincial Key Lab of Fine Chemistry, Hainan University, Haikou, Hainan 570228, P.R. China

E-mail address: xh@ujs.edu.cn, lihm@ujs.edu.cn

The graphene-like MoS_2/Ag_3VO_4 composites exhibited remarkable enhanced photocatalytic activities on the photodegradation of dyes within a short time than that of the individual Ag_3VO_4.